

See discussions, stats, and author profiles for this publication at: <https://www.researchgate.net/publication/225583307>

Leaf Surface Wettability and Implications for Drop Shedding and Evaporation from Forest Canopies

Article in *Pure and Applied Geophysics* · May 2011

DOI: 10.1007/s00024-011-0330-2

CITATIONS

22

READS

156

4 authors:



Wilfried Konrad

University of Tuebingen

60 PUBLICATIONS 833 CITATIONS

[SEE PROFILE](#)



Martin Ebner

University of Tuebingen

36 PUBLICATIONS 468 CITATIONS

[SEE PROFILE](#)



Christopher Traiser

University of Tuebingen

31 PUBLICATIONS 457 CITATIONS

[SEE PROFILE](#)



Anita Roth-Nebelsick

State Museum of Natural History Stuttgart

143 PUBLICATIONS 2,091 CITATIONS

[SEE PROFILE](#)

Some of the authors of this publication are also working on these related projects:



Textiler Feuchttransfer [View project](#)



AiF 19808 N «Textiler Feuchttransfer» – Biomimetisch-simulationsbasierte Textilstrukturen für neuartige Lösungen zur Feuchteverdunstung, -kondensation und -versorgung von Pflanzen im Gewächshausgartenbau. [View project](#)

Leaf surface wettability and implications for drop shedding and evaporation from forest canopies

W. Konrad^{1,*}, M. Ebner¹ and A. Roth-Nebelsick²

¹University of Tübingen, Institute for Geoscience, Sigwartstrasse 10, D-72076 Tübingen, Germany

²State Museum of Natural History, Rosenstein 1, 70191 Stuttgart, Germany

Abbreviated title: Leaf surface wettability

Keywords: wettability, canopy, contact angle, contact angle hysteresis, hydrology, interception

Wettability and retention capacity of leaf surfaces are parameters that contribute to interception of rain, fog or dew by forest canopies. Contrary to common expectation, hydrophobicity or wettability of a leaf do not dictate the stickiness of drops to leaves. Crucial for the adhesion of drops is the contact angle hysteresis, the difference between leading edge contact angle and trailing edge contact angle for a running drop. Other parameters that are dependent on the static contact angle are the maximum volume of drops that can stick to the surface and the persistence of an adhering drop with respect to evaporation. Adaption of contact angle and contact angle hysteresis allow to pursue different strategies of drop control, for example efficient water shedding or maximum retention of adhering water. Efficient water shedding is achieved if contact angle hysteresis is low. Retention of (isolated) large drops requires a high contact angle hysteresis and a static contact angle of 65.5° , while maximum retention by optimum spacing of drops necessitates a high contact angle hysteresis and a static contact angle of 111.6° . Maximum persistence with respect to evaporation is obtained if the static contact angle amounts to 77.5° , together with a high contact angle hysteresis. It is to be expected that knowledge of these parameters can contribute to the capacity of a forest to intercept water.

1. Introduction

A significant amount of water that precipitates within canopies as rain, fog or dew is intercepted by the forest canopy. Interception comprises various processes that occur after the water has come into contact with plant surfaces: evaporation of water retained inside the canopy (interception loss), down drip off the canopy (drip) and down flow along the stems (stemflow). Canopy interception is a process of considerable importance for the hydrological cycle since annual interception losses in forests can amount to more than a quarter of total rainfall (Hörman et al. 1996, Dingman 2002). Determination of hydrological input by fog is partially very difficult due to the exact determination of interception.

*Corresponding author: wilfried.konrad@uni-tuebingen.de

The actual rate of interception loss is dependent on various factors, such as forest structure, fog or rain intensity and meteorological parameters. Precise knowledge on interception losses are of substantial importance for predicting and modeling hydrological processes, such as effects of woodland, climate or land cover on water resources (Gash et al. 1980, Calder 1990, Aboal et al. 1999, Muzylo et al. 2009). The maximum amount of water that can be temporarily hold by a canopy is mainly distributed between bark and leaves (Herwitz 1985). For the leaves, the amount of stored water is a function of Leaf Area Index (LAI), however with substantial interspecific differences (Aston 1979). Besides leaf area, wettability of the leaves is expected to be important. Wettability describes the behaviour of water after coming in contact with a surface. Water repellent surfaces are hydrophobic, and droplets upon these surfaces develop spherical forms with contact angles $> 90^\circ$ (Calies and Quéré 2005). On hydrophilic surfaces, droplets attain contact angles $< 90^\circ$. Complete wetting leads to the spreading of drops into films. Water repellency differs substantially between upper and lower side of leaves, between species and between forest types (Holder 2007).

Wettability and the resulting contact angle also influences the gliding angle, that is, the angle of inclination of an object that leads to the rolling off of drops lying upon an object or being attached to the underside of the object. Wettability of a leaf depends on the chemical nature of the leaf waxes, as well as on structures of the leaf surface, including papillae and trichomes (Barthlott and Neinhuis 1997, Shirtcliffe et al. 2009). It is intuitively expected that the more water repellent a surface is, the lower is the gliding angle. This would mean that a low inclination would be sufficient to remove drops from the object, and species with water repellent leaves would therefore show a lower storage capacity for rain interception than a species with more hydrophilic leaves.

However, the gliding angle is not only dependent on wettability. Rather, contact angle hysteresis governs the gliding behavior of droplets on a surface (Quéré 2008), that is, the difference between the developing contact angle when a droplet moves forwards (advancing contact angle) or backwards (receding contact angle). For example, petals can be very sticky with respect to droplet behavior despite their low wettability (Feng et al. 2008). In this contribution we consider the interrelationship between wettability and contact angle hysteresis and gliding behaviour of drops attached to surfaces. In particular, we will address the following questions: Which contact angle leads to (i) a maximum storage capacity of a surface with respect to sitting or hanging drops, and (ii) a maximum persistence of drops with respect to evaporation (under a given humidity and temperature.)

2. Basic properties of droplets attached to a plane

In this section we derive volumes and areas of droplets attached to a horizontal or inclined plane and the surface and gravitational forces acting on them.

2.1. Droplet hanging down from a horizontal plane

We consider a droplet hanging down from a horizontal plane under its own weight (Fig. 1). Assuming that the droplet is shaped as a segment of a sphere of radius R and that the contact angle formed between droplet and substrate is θ the volume of the spherical segment amounts to

$$V = \frac{\pi R^3}{3} (1 - \cos \theta)^2 (2 + \cos \theta) = \frac{\pi s^3}{3} \frac{(1 - \cos \theta)^2 (2 + \cos \theta)}{\sin^3 \theta} \quad (1)$$

The second version is a result of the substitution $s = R \sin \theta$, where s denotes the radius of the circle which forms the contact line where water, air and the solid of the plane meet. The surface area of the

droplet is the sum $M + S$, where

$$S = \pi R^2 \sin^2 \theta = \pi s^2 \quad (2)$$

$$M = 2\pi R^2(1 - \cos \theta) = \frac{2\pi s^2}{1 + \cos \theta} \quad (3)$$

S denotes the attachment area between drop and plane and M denotes that part of the droplet surface which is in contact with air.

As long as the droplet is pending the force due to its weight is compensated by the force which originates from the surface tension of the water/air-interface at the contact line (see Figure 1). The infinitesimal force arising from an infinitesimal element of this circle can be decomposed into a horizontally and a vertically oriented component. Integrating along the contact line (i.e. the circle) the integral of the horizontal force component vanishes because of the axial symmetry of the situation while the vertical component of the tension force adds up to

$$F_\sigma = 2\pi \sigma s \sin \theta \quad (4)$$

where σ denotes the surface tension between water and air. For a droplet with maximum volume F_σ should be balanced by the gravitational force

$$F_g = \rho g V \quad (5)$$

caused by the droplet's weight. Exploiting expression (1) and then solving $F_g = F_\sigma$ for the radius s_m of the contact circle corresponding to a maximum volume droplet we arrive at

$$s_m = \frac{l(1 + \cos \theta)}{\sqrt{2 + \cos \theta}} \quad (6)$$

The quantity

$$l := \sqrt{\frac{6\sigma}{\rho g}} \approx 6.60 \times 10^{-3} \text{ m} \quad (7)$$

depends merely on the natural constants surface tension (between air and water) $\sigma \approx 72 \times 10^{-3} \text{ N/m}$, the gravitational acceleration $g \approx 10 \text{ m/s}^2$ and the density of water $\rho \approx 10^3 \text{ kg/m}^3$. Thus, it represents a characteristic length of the problem. (In the literature the expression $\sqrt{\sigma/(\rho g)}$ is known as the capillary constant.) From $s = R \sin \theta$ and (6) we find

$$R_m = \frac{l(1 + \cos \theta)}{\sin \theta \sqrt{2 + \cos \theta}} \quad (8)$$

and (upon insertion of (6) into expression (1)) we obtain the maximum volume V_m of the droplet:

$$V_m = \frac{\pi l^3}{3} \frac{(1 + \cos \theta) \sin \theta}{\sqrt{2 + \cos \theta}} \quad (9)$$

Notice that although $s_m(\theta)$, $R_m(\theta)$ and $V_m(\theta)$ represent a droplet which is — due to its weight — on the verge of falling down these functions depend still on the contact angle θ (see Figure 2). Hence, we may

calculate the contact angle(s) where they attain their maxima. Interestingly, the maxima of $s_m(\theta)$ and $V_m(\theta)$ do *not* coincide. We rather find:

$$\theta_{s_m} = 0^\circ : \quad s_m(\theta_{s_m}) = \frac{2\sqrt{3}}{3} l \approx 7.62 \times 10^{-3} \text{ m} \quad (10)$$

$$\theta_{V_m} = \arccos(\sqrt{2} - 1) \approx 65.5^\circ : \quad s_m(\theta_{V_m}) = \left(\sqrt{2}(\sqrt{2} - 1) \sqrt{\sqrt{2} + 1} \right) l \approx 6.01 \times 10^{-3} \text{ m} \quad (11)$$

$$V_m(\theta_{V_m}) = \frac{2\pi(\sqrt{2} - 1)}{3} l^3 \approx 250 \times 10^{-9} \text{ m}^3 \quad (12)$$

2.2. Droplet and inclined plane

In conjunction with horizontally oriented planes only hanging droplets are interesting, because the vertically directed force of gravitation has no horizontal component which could push around droplets attached to the upper side of the plane. If the plane is inclined with respect to the horizontal the situation changes. Hence, we consider now both hanging and sitting droplets.

2.2.1. Forces acting on a hanging droplet, conditions for detachment and downslide

Consider a droplet of given volume V hanging down from a plane which is inclined against the horizontal by an angle α (Fig. 3). If α is increased, the shape of the droplet deviates — at first slightly, then increasingly — from being a segment of a sphere. The droplet as a whole, however, does not move. Eventually — when a critical angle of inclination has been reached — the droplet either starts to slide down or it detaches from the plane and falls down. Similarly as in Section 2.2.1 (expression (6)) we would like to find a relation between the “system defining” variables like s , θ and α which characterises the onset of slide or detachment.

Experimentally, it has been found that at the critical inclination the contact angle θ assumes along the “upstream” segment of the contact circle the receding value θ_r . At the “downstream” segment of the contact circle, however, the advancing contact angle θ_a is realised.

Decomposition of \mathbf{F}_g and \mathbf{F}_σ into components parallel and normal to the inclined plane (Figure 3) leads to two conditions:

- (a) Downslide of the droplet sets in when the tangential component of gravity surmounts the tangential component of the surface tension

$$F_{g,t} \equiv \rho g V \sin \alpha \geq k \sigma w (\cos \theta_r - \cos \theta_a) \equiv F_{\sigma,t} \quad (13)$$

w denotes the maximum halfwidth of the droplet. The detailed theory of a sliding droplet is rather involved (see Extrand and Kumagai 1995, Petrissans and Cscapo 2003, Podgorski et al. 2001, Dimitrakopoulos and Higdon 1998, Dimitrakopoulos and Higdon 1999, Glasner 2007). Most authors agree on the structure of equation (13) but disagree on the value of the numerical constant k to which various values in the range $k = \pi/4 \dots 2$ have been assigned. Moreover, k depends also on the shape of the droplet.

- (b) Detachment of the droplet from the plane occurs if the normal gravity component is greater than the normal component of the surface tension

$$F_{g,n} \equiv \rho g V \cos \alpha \geq \frac{\pi}{2} k \sigma w (\sin \theta_r + \sin \theta_a) \equiv F_{\sigma,n} \quad (14)$$

As they stand, equations (13) and (14) are of limited use because they contain the droplet volume V which is difficult to obtain experimentally. If, however, the shape of the droplet deviates not too much from a segment of a sphere, the contact line is a circle with radius s and we can use equation (1) to express V in terms of s and the contact angle θ which is in this context defined as the arithmetic mean of the receding and the advancing contact angle:

$$\theta = \frac{\theta_a + \theta_r}{2} \quad (15)$$

Moreover, if the droplet is quasi-spherically shaped, we may conclude $w = s$ and $k = 2$ (see Petrisans), which we shall assume in the sequel. Then, insertion of (1) into (13) and (14) allows to solve these expressions for the contact circle radii s at which the equals signs in (13) and (14) are realised. Employing the definition

$$\chi := \frac{\theta_a - \theta_r}{2} \quad (16)$$

and the relations

$$\begin{aligned} \cos x - \cos y &= -2 \sin \frac{x+y}{2} \sin \frac{x-y}{2} \\ \sin x - \sin y &= 2 \sin \frac{x+y}{2} \cos \frac{x-y}{2} \end{aligned} \quad (17)$$

conditions (a) and (b) can be stated as follows:

(a) Downslide sets in if $s > s_\sigma$, where

$$s_\sigma := \frac{l(1 + \cos \theta)}{\sqrt{2 + \cos \theta}} \sqrt{\frac{2}{\pi} \frac{\sin \chi}{\sin \alpha}} \quad (18)$$

(b) Detachment occurs if $s > s_g$, where

$$s_g := \frac{l(1 + \cos \theta)}{\sqrt{2 + \cos \theta}} \sqrt{\frac{\cos \chi}{\cos \alpha}} \quad (19)$$

Meaningful ranges of θ and χ are: $0 \leq \theta \leq \pi$ and $0 \leq \chi \leq \pi/2$. The latter is equivalent to $0 \leq \theta_a - \theta_r \leq \pi$. Whether a droplet of contact radius s detaches itself from or slides down along the inclined plane depends on the relation between s , s_σ and s_g : For $s > s_g > s_\sigma$, sliding sets in, for $s > s_\sigma > s_g$, however, detachment occurs.

The relation between s_σ and s_g reduces via (18) and (19) to a relation between α and χ :

$$s_\sigma < s_g \quad \Longleftrightarrow \quad \tan \alpha > \frac{2}{\pi} \tan \chi \quad (\text{downslide if } s > s_g) \quad (20)$$

$$s_\sigma > s_g \quad \Longleftrightarrow \quad \tan \alpha < \frac{2}{\pi} \tan \chi \quad (\text{free fall if } s > s_\sigma) \quad (21)$$

2.2.2. Critical volume of a hanging droplet, contact angle and gliding angle

Combination of (18) and (19) with (1) results in an expression for the critical droplet volume:

$$V_c := \left\{ \frac{\pi l^3}{3} \frac{(1 + \cos \theta) \sin \theta}{\sqrt{2 + \cos \theta}} \right\} \times \begin{cases} \sqrt{\left(\frac{2}{\pi} \frac{\sin \chi}{\sin \alpha} \right)^3} & \text{if } \tan \alpha > \frac{2}{\pi} \tan \chi \quad (\text{downslide if } V > V_c) \\ \sqrt{\left(\frac{\cos \chi}{\cos \alpha} \right)^3} & \text{if } \tan \alpha < \frac{2}{\pi} \tan \chi \quad (\text{free fall if } V > V_c) \end{cases} \quad (22)$$

The condition that a pending droplets starts to move (either by downslide or by detachment) can be stated as $V > V_c$. Critical droplet volumes $V_c(\alpha)$ for a few combinations of θ and χ are depicted in Fig. 4. This figure illustrates also that the curves $V_c(\alpha)$ exhibit maxima at $\alpha_m = \arctan\left(\frac{2}{\pi} \tan \chi\right)$. Notice, that the expression in braces equals the volume V_m (defined in (9)) which emerged in the context of droplets hanging down from a horizontal plane. In order to clarify the role of χ with respect to droplet motion we divide the equation $V = V_c$, which separates immobile ($V < V_c$) and falling or sliding ($V > V_c$) droplets, by V_m (see (9)). It becomes then feasible to reformulate the conditions for droplet (im-)mobility in terms of relations between the inclination angle α and the half-difference of advancing and receding contact angle χ : Depending on the value of V/V_m , the pair of curves

$$\alpha = \begin{cases} \arcsin\left(\frac{2}{\pi}\left(\frac{V_m}{V}\right)^{\frac{2}{3}} \sin \chi\right) & \text{if } \tan \alpha > \frac{2}{\pi} \tan \chi \\ \arccos\left(\left(\frac{V_m}{V}\right)^{\frac{2}{3}} \cos \chi\right) & \text{if } \tan \alpha < \frac{2}{\pi} \tan \chi \end{cases} \quad (23)$$

divides the (χ, α) -plane into either (a) three sections, if V is in the interval $0 < V \leq (2/\pi)^{3/2} V_m \approx 0.5 V_m$ (Fig. 5(a)), or (b) two sections, if $(2/\pi)^{3/2} V_m < V < V_m$ applies (Fig. 5(b)). (χ, α) -pairs lying between the two curves indicate that a droplet of volume V remains immobile. Droplets (of this same volume) characterised by a (χ, α) -pair above/left of the upper curve slide down, droplets below/right of the lower curve detach from the plane and fall down.

The important conclusion is, that droplets of a given volume that fall into category (a) can be made to adhere to an arbitrarily inclined plane if χ can be adjusted appropriately, whereas droplets belonging to category (b) cannot be kept immobile for every inclination $0 < \alpha < \pi/2$, even if χ can be arbitrarily chosen.

It is thus justified to identify the upper expression of (23) with the gliding angle γ (the angle of inclination of an object that leads to the rolling off of drops lying upon the object) and its lower counterpart with an “detachment angle” δ (the angle of inclination of an object that leads to the detachment of drops from the object). Upon insertion of (9) expression (23) transforms to

$$\gamma := \arcsin\left(\sqrt[3]{\frac{8}{9\pi}} \left(\frac{l^3}{V}\right)^{\frac{2}{3}} \frac{\sin^2 \theta \sin \chi}{\sqrt[3]{(1 - \cos \theta)^2 (2 + \cos \theta)}}\right) \quad (24)$$

$$\delta := \arcsin\left(\sqrt[3]{\frac{\pi^2}{9}} \left(\frac{l^3}{V}\right)^{\frac{2}{3}} \frac{\sin^2 \theta \cos \chi}{\sqrt[3]{(1 - \cos \theta)^2 (2 + \cos \theta)}}\right) \quad (25)$$

where it is implicit that the condition $V \leq V_m$ should be fulfilled, if (24) and (25) are applied to hanging droplets. If so, the condition that a droplets starts to slide down can be expressed by the statement $\alpha > \gamma$, and the condition that a droplets starts to detach from the plane is equivalent to $\alpha < \delta$. Droplet immobility is realised where $\gamma < \alpha < \delta$ applies (cf. Fig. 5). If $\delta > \gamma$ is valid (as in the upper, right part of Fig. 5(b)) immobile droplets can not exist.

2.2.3. Sitting droplet, conditions for downslide

A droplet sitting on the upper surface of an inclined leaf cannot choose between “downslide” and “free fall” (although free fall may eventually become an option, if the droplet reaches the leaf margin). Thus,

the lower line of (22) and “detachment condition” (25) become void. The condition that a droplet starts to move can be expressed either by the statement $V > V_c$, where

$$V_c = \left\{ \frac{\pi l^3}{3} \frac{(1 + \cos \theta) \sin \theta}{\sqrt{2 + \cos \theta}} \right\} \sqrt{\left(\frac{2 \sin \chi}{\pi \sin \alpha} \right)^3} \quad (26)$$

or by the condition $\gamma > \alpha$ (see (24)) which is in this case valid without the restriction $V \leq V_m$. Similarly as in the case of the hanging droplet, an increase of droplet volume brings about a drastic decrease of the (χ, α) -area wherein droplets remain sessile (equation (24) and Fig. 6).

The main result of this section concerns the dependence of the critical volume $V_c(\theta, \chi, \alpha)$ on the contact angle θ , the half-difference of advancing and receding contact angle χ and the inclination α of the plane to which the hanging or sitting droplet is attached (cf. Figs. 4 and 5):

- The critical volume shows a maximum with respect to θ at $\theta_{V_m} = \arccos(\sqrt{2} - 1) \approx 65.5^\circ$ (for constant values of χ and α , Fig 2(b) illustrates — apart from a constant factor — the θ -dependence of $V_c(\theta, \chi, \alpha)$).
- For sitting droplets (and for hanging droplets, provided $\tan \alpha > \frac{2}{\pi} \tan \chi$) the critical volume increases with increasing χ .
- For sitting droplets (and for hanging droplets, provided $\tan \alpha > \frac{2}{\pi} \tan \chi$) the critical volume decreases with increasing α .

Consequently, if a leaf surface wants to dispose of hanging or sitting water droplets for a given leaf inclination α , it has to options: (i) It may minimise contact angle hysteresis (i.e. aiming for $\chi \rightarrow 0$), it can try to produce a contact angle which either much smaller or much larger than the value $\theta_{V_m} \approx 65.5^\circ$ for which V_c attains its maximum. Minimising χ is probably the more promising choice, since it has — according to Fig. 4 or equation (22) — the effect of shifting the maxima of the V_c -curves (which exist for hanging droplets only) to smaller values of α , hereby enhancing the tendency to detach or slip down of a droplet.

Contrariwise, if a leaf wants to store much water it should try to arrange for (i) a large angle χ and (ii) a contact angle close to $\theta_{V_m} \approx 65.5^\circ$.

3. Maximum storage capacity and optimum spacing of droplets

Consider a leaf which wants to store as much water as possible in the form of droplets attached to its lower or upper surface. Two questions arise: (i) Which geometric pattern should the droplets form, and, (ii) exists an optimum contact angle?

Obviously, the optimum pattern is realised by partitioning the leaf surface into hexagons and “inscribing” into each of them one droplet. If the contact angle is in the range $0 \leq \theta \leq \pi/2$ the contact circle represents the greatest lateral extension of the droplet, hence the radius of the hexagon’s incircle should equal s . For $\pi/2 \leq \theta \leq \pi$, however, $R > s$, thus the incircle radius should equal R . The respective areas amount to

$$A_{hex} = \begin{cases} 2\sqrt{3}s^2 & \text{if } 0 \leq \theta \leq \pi/2 \\ 2\sqrt{3}R^2 & \text{if } \pi/2 \leq \theta \leq \pi \end{cases} \quad (27)$$

In order to calculate the contact angle related to maximum storage capacity, we form the quantity $\mu := [\text{maximum water volume stored in one droplet}]/[\text{leaf area required for one droplet}]$.

3.1. Horizontal plane

Recalling that the volume of hanging droplets exhibits a maximum value V_m which depends according to (9) on the contact angle θ , we find from (9), (6), (8) and (27)

$$\mu_m := \begin{cases} \left(\frac{l\pi\sqrt{3}}{18} \right) \frac{\sin \theta \sqrt{2 + \cos \theta}}{1 + \cos \theta} & \text{if } 0 \leq \theta \leq \pi/2 \\ \left(\frac{l\pi\sqrt{3}}{18} \right) \frac{\sin^3 \theta \sqrt{2 + \cos \theta}}{1 + \cos \theta} & \text{if } \pi/2 \leq \theta \leq \pi \end{cases} \quad (28)$$

It appears that μ_m features a maximum with respect to θ which is located at

$$\theta_{\mu_m} = \pi - \arctan \left(\frac{\sqrt{10\sqrt{10} + 26}}{3} \right) \approx 111.6^\circ \quad (29)$$

i.e. in the hydrophobic range of contact angles. Insertion into (28) produces

$$\mu_{m,max} = \left(\frac{l\pi\sqrt[4]{1125}}{2250} \right) \sqrt{(\sqrt{10} - 1)^3 (\sqrt{5} + \sqrt{2})} \approx 0.49 l \quad (30)$$

Since droplets sitting on a horizontal plane can not be detached by gravitation, their volume is — in principle — unlimited, that is, both s and R can be increased (almost) indefinitely. Forming $\mu = V/A_{hex}$ from expressions (1) and (27) results in

$$\mu = \begin{cases} s \left(\frac{\pi\sqrt{3}}{18} \right) \frac{(1 - \cos \theta)^2 (2 + \cos \theta)}{\sin^3 \theta} & \text{if } 0 \leq \theta \leq \pi/2 \\ R \left(\frac{\pi\sqrt{3}}{18} \right) (1 - \cos \theta)^2 (2 + \cos \theta) & \text{if } \pi/2 \leq \theta \leq \pi \end{cases} \quad (31)$$

The absence of θ -dependent upper limits for s and R effects the θ -dependence of μ (compared to μ_m): Other than (28), expression (31) exhibits no maximum with respect to θ .

3.2. Inclined plane

Assuming that the shape of droplets attached to an inclined plane deviates not much from a segment of a sphere, expression (31) is valid, provided that $V < V_c$ (where V and V_c are defined in (1) and (22), respectively).

In the limit $V = V_c$, expression (27) assumes upon use of (31) (22) (resp. (26)), (18) (19) and (27) the form

$$\mu_c := \frac{V_c}{A_{hex}} = \mu_m(\theta) \times \begin{cases} \sqrt{\left(\frac{2}{\pi} \frac{\sin \chi}{\sin \alpha} \right)^3} & \text{if } \tan \alpha > \frac{2}{\pi} \tan \chi \quad (\text{downslide if } V > V_c) \\ \sqrt{\left(\frac{\cos \chi}{\cos \alpha} \right)^3} & \text{if } \tan \alpha < \frac{2}{\pi} \tan \chi \quad (\text{free fall if } V > V_c) \end{cases} \quad (32)$$

Notice that the θ -dependence of μ_c is contained in $\mu_m(\theta)$ (as given in (28)). Therefore, it shares with $\mu_m(\theta)$ the maximum described in (29). As it stands, expression (32) is valid for hanging droplets of critical (maximum) volume V_c . Sitting droplets of volume V_c are represented by the upper line of (32), only.

4. Lifetime of a droplet

In section 3 we explored the maximum storage capacity of a leaf. In this section we evaluate (i) the lifetime of a droplet subjected to evaporation, and (ii) whether its lifetime depends on its radius and on the leaf contact angle.

4.1. Horizontal plane

A droplet which is attached to a leaf loses water by evaporation through the droplet's water/air interface M (see (3)). This particle loss leads to a decrease of the droplet volume V , according to

$$-\frac{dV}{dt} = j_M M \quad (33)$$

For what follows, we assume that the evaporation flux j_M is a constant with respect to t and θ . Applying textbook thermodynamics (e.g. Reif 1974, Atkins 1998), j_M can — under these assumptions — be expressed as

$$j_M = D_{wv} V_{wv} \left(\frac{c_{sat} - c_{wv}}{b} \right) \quad (34)$$

D_{wv} denotes the diffusional constant of water vapour in air, V_{wv} the molar volume of water vapour, b is the thickness of the boundary layer surrounding the leaf. c_{wv} denotes the atmospheric molar concentration of water vapour, and c_{sat} the saturation value related to it.

Employing the differentiation rule $dV(s)/dt = (dV/ds)(ds/dt)$ and expressions (1), (3) and (2), equation (33) becomes after a few rearrangements a simple differential equation for $s(t)$

$$-\frac{ds}{dt} = \frac{2j_M(1 + \cos \theta)}{(2 + \cos \theta) \sin \theta} \quad (35)$$

with the solution

$$s(t) = s_0 - \frac{2j_M(1 + \cos \theta)}{(2 + \cos \theta) \sin \theta} t \quad (36)$$

where s_0 denotes the radius of the contact line at time $t = 0$ when evaporation and/or absorption set in (cf. Fig. 1). The lifetime τ of the droplet is obtained by letting $s = 0$ in (36) and solving for t ,

$$\tau = \frac{(2 + \cos \theta) \sin \theta}{2j_M(1 + \cos \theta)} s_0 \quad (37)$$

If the initial radius of the contact line attains the value s_m (corresponding to the maximum volume $V_m(\theta)$ of a hanging droplet), the droplet's lifetime becomes

$$\tau_m = \frac{l \sin \theta \sqrt{2 + \cos \theta}}{2j_M} \quad (38)$$

It is interesting to calculate the contact angle θ_τ for which the lifetime τ_m becomes a maximum. It turns out that it depends neither on l nor on j_M . Its value amounts to

$$\theta_\tau := \arccos\left(\frac{\sqrt{7}-2}{3}\right) \approx 77.5^\circ \quad (39)$$

which is in the hydrophilic range of contact angles. Upon insertion of θ_τ into τ_m we find

$$\tau_{m,max} = \frac{l}{j_M} \frac{\sqrt{10+7\sqrt{7}}}{3\sqrt{6}} \approx 0.73 \frac{l}{j_M} \quad (40)$$

An explicit expression for $V(t)$ results from insertion of (36) into (1):

$$V(t) = \frac{\pi}{3} (2 + \cos \theta) \sqrt{1 - \cos \theta} \left\{ \frac{s_0}{\sqrt{1 + \cos \theta}} - \frac{2j_M}{(2 + \cos \theta) \sqrt{1 - \cos \theta}} t \right\}^3 \quad (41)$$

4.2. Inclined plane

If the plane is inclined, the basic equation (33) remains valid both for hanging and sitting droplets. Treating the droplets as quasi-spherical segments the same reasoning as above applies with the same results regarding the t -dependance of s and V and the droplet lifetime (equations (36), (41) and (37), respectively).

In the case of hanging droplets we have to take into account that the initial value s_0 of the contact circle should — due to the inclination of the leaf — fulfill the conditions $s_0 < s_\sigma$ and $s_0 < s_g$ (see (18) and (19)).

If a hanging droplet is initially of maximum volume (i.e. $s_0 = s_\sigma$ or $s_0 = s_g$, depending on the values of the inclination angle α and on the half-difference of advancing and receding contact angle χ), τ simplifies to

$$\tau_c = \left\{ \frac{l \sin \theta \sqrt{2 + \cos \theta}}{2j_M} \right\} \times \begin{cases} \sqrt{\frac{2}{\pi} \frac{\sin \chi}{\sin \alpha}} & \text{if } \tan \alpha > \frac{2}{\pi} \tan \chi \\ \sqrt{\frac{\cos \chi}{\cos \alpha}} & \text{if } \tan \alpha < \frac{2}{\pi} \tan \chi \end{cases} \quad (42)$$

where the expression in braces is just τ_m , the lifetime of a droplet hanging from a horizontal plane.

5. Discussion

The easiness with which water drops roll off a surface is mainly dependent on the contact angle hysteresis of a surface, and not on the static contact angle. The smaller the contact angle hysteresis the easier a drop will roll off the surface. Thus, hydrophobicity does not necessarily lead to a low stickiness of drops to the surface. To determine the stickiness of drops to surfaces it is not sufficient to measure the static contact angle θ . It is necessary to measure also χ . Potential benefits of efficient shedding of drops for a leaf are frequently discussed with respect to self cleaning. Pathogens, such as fungal spores, are easily washed off then or are prevented from germination on the constantly dry surface (Barthlott and Neinhuis 1997). If a plant species pursues the strategy to efficiently get rid of

water drops upon its surface, it should minimize χ . This quantity is usually influenced by the often heterogeneous nature of surfaces, with respect to surface micro/nanostructure and/or local contact angle variations (Quéré 2008). In leaves, these surface effects will be mostly created by cuticle wax structures and/or trichomes.

Another benefit has to do with photosynthesis since the development of a water film above stomata, the gas exchange pores of a leaf, is deleterious for photosynthesis. To keep stomata free from a water film, it is beneficial — besides to get rid of the drops by a low χ — to reduce the contact area between a droplet and the surface. Consequently, high water repellency, together with low stickiness for drops, is expected for species in foggy habitats and especially for stomatous leaf sides (frequently the abaxial side). Holder (2007) found that for different forest species θ tended to be unexpectedly low for many cloud forest species. He discussed this result as being caused by the high erosion of cuticle waxes due to intense precipitation. However, since χ was not determined in Holder's study, leaves may pursue also other strategies by their surface properties than easy shedding of spherical drops. For example, it may be speculated that fog harvesting species are interested in collecting large drops before they roll off the leaf and fall to the ground. Fog drip can be an important source of water input (Feng et al. 2008). The shedding of large drops is expected to be more efficient in wetting the soil around the plant than the shedding of many small or very small droplets because large drops have a higher potential for throughfall. Furthermore, due to their low surface-to-volume-ratio, they will resist evaporation much stronger than small droplets. Maximum drop size can be achieved with a $\theta \approx 65.5^\circ$. A good ability for water retention may have also other beneficial aspects. There are various plants that are able to absorb water via the leaves. This was unambiguously demonstrated for Californian redwoods (Burgess and Dawson 2004), but also indicated for other species (Breshears et al. 2008). If water absorption by leaves represents an important water source for a species, then it should be expected that both a good wetting behavior (low θ and a high χ leading to a high persistence of the water on the leaf) is beneficial. This would then prolong the water amount and the time interval available for absorption. The highest leaf storage capacity of a leaf would be obtained with a contact angle of $\theta \approx 111.6^\circ$ and a high χ . For maximum persistence of a drop under given meteorological conditions, the contact angle should amount to $\theta \approx 77.5^\circ$.

Furthermore, nutrient input via aerosols are important for many ecosystems, and it was shown that hygroscopic mineral salts can be found upon leaf surfaces (Burkhardt 2010). Absorption not only of water but also of minerals solved in leaf surface water may therefore be of substantial importance for species living on nutrient-poor soils (Burkhardt 2010) and a good water retention should be also beneficial in these cases.

Leaf surface properties do not only affect the hydrological cycle via canopy interception but can also be important for the plant. The ecophysiological interrelationships between leaf surface and drops can be manifold, and may additionally be changed by external factors, such as dust particles, abrasion or insect-mediated structural changes. Furthermore, the mechanical impacts of wind currents or animal activities upon leaves will frequently be sufficient to lead to detachment of drops that otherwise would be attached quite firmly to the leaf surface. The consequences and impacts of the behaviour of deposited drops upon leaf surfaces are complex for a considered species and depend on its habitat, ecological niche and other ecophysiological traits. Often, an interrelationship to any vital function cannot be provided. The ability of hydrophobic petals, for example, to retent a water droplet firmly, even if upside down ("Petal Effect") (Feng et al. 2008), can presently not be explained as being of any adaptive value. Considering the various complex interrelationships of leaves with their environment, the interaction of leaf surfaces with water is a fascinating and important topic that deserves further attention.

References

- Aboal, J.R., Jiménez, M.S., Morales, D., Hernández, J.M. (1999), Rainfall interception in laurel forest in the Canary Islands. *Agricultural and Forest Meteorology* 97, 73–86.
- Aston, A.R. (1979), Rainfall interception by eight small trees. *Journal of Hydrology* 42, 383–396.
- Atkins, P., *Physical Chemistry* (W.H. Freeman, New York 1998).
- Barthlott, W., Neinhuis, C. (1997), Purity of the sacred lotus, or escape from contamination in biological surfaces. *Planta* 202, 1–8.
- Breshears, D., McDowell, N.G., Goddard, K. L., Dayem, K. E., Martens, S. N., Meyer, C. W., Brown, K. M. (2008), Foliar absorption of intercepted rainfall improves woody plant water status most during drought. *Ecology* 89, 41–47.
- Burgess, S.S.O., Dawson, T.E., (2004), The contribution of fog to the water relations of *Sequoia sempervirens* (D. Don): foliar uptake and prevention of dehydration. *Plant, Cell and Environment* 27, 1023–1034.
- Burkhardt, J. (2010), Hygroscopic particles on leaves: nutrients or desiccants? *Ecological Monographs*, 80, 369–399.
- Calder, I. (1990), *Evaporation in the uplands*. John Wiley and sons Inc., Chichester. 149 pp.
- Calies, M., Quéré, D. (2005), On water repellency. *Soft Matter* 1, 55–61.
- Dimitrakopoulos, P., and Higdon, J.J.L. (1998), On the displacement of three-dimensional fluid droplets from solid surfaces in low-Reynolds-number shear flows, *J. Fluid Mech.* 377, 189–222.
- Dimitrakopoulos, P., and Higdon, J.J.L. (1999), On the gravitational displacement of three-dimensional fluid droplets from inclined solid surfaces, *J. Fluid Mech.* 395, 181–209.
- Dingman, S., *Physical hydrology* (Prentice Hall, Upper Saddle River 2002)
- Extrand, C.W., and Kumagai, Y., (1995), Liquid drops on a inclined plane: the relation between contact angles, drop shape, and retentive force. *Journal of Colloid and Interface Science* 170, 515–521.
- Feng, L., Zhang, Y.A., Xi, J.M., Zhu, Y., Wang, N., Xia, F., Jiang, L. (2008), Petal effect: Two major examples of the Cassie-Baxter model are the “Petal effect” and “Lotus effect”. A superhydrophobic state with high adhesive force. *Langmuir* 24, 4114–4119.
- Gash, J.H.C. (1979), An analytical model of rainfall interception by forests. *Journal of Hydrology* 105, 43–55.
- Glasner, K.B. (2007), The dynamics of pendant droplets on a one-dimensional surface, *Physics of Fluids* 19, 102104.
- Herwitz, S.R. (1985), Interception storage capacities of tropical rainforest canopy trees. *Journal of Hydrology* 77, 237–252.
- Hörman, G., Branding, A., Clemen, T., Herbst, M., Hinrichs, A. (1996), Calculation and simulation of wind controlled canopy interception of beech forest in Northern Germany. *Agricultural and Forest Meteorology* 79, 131–148.
- Holder, C.D. (2007), Leaf water repellency of species in Guatemala and Colorado (USA) and its significance to forest hydrology studies. *Journal of Hydrology* 336, 147–154.
- Muzylo, A., Llorens, P., Valente, F., Keizer, J.J., Domingo, F., Gash, J.H.C. (2009), A review of rainfall interception modelling. *Journal of Hydrology* 370, 191–206.
- Petrissans, M., and Cscapo, E. (2003), Retention of glycerol sessile drop on MDF wood material, *Holz als Roh- und Werkstoff*, 61, 12–116.
- Podgorski, T., Flesselles, J.-M., and Limat, L. (2001), Corners, Cusps, and Pearls in Running Drops, *Phys. Rev. Lett.* 87, 036102.
- Quéré, D. (2008), Wetting and roughness. *Annual Review of Materials Research* 38, 71–99.
- Reif, F., *Fundamentals of statistical and thermal physics* (McGraw-Hill, New York 1974).

Shirtcliffe, N.J., McHale, G., Newton, M.I. (2009), Learning from superhydrophobic plants: The use of hydrophilic areas on superhydrophobic surfaces for droplet control. *Langmuir* 25, 14121–14128.

A. Figures

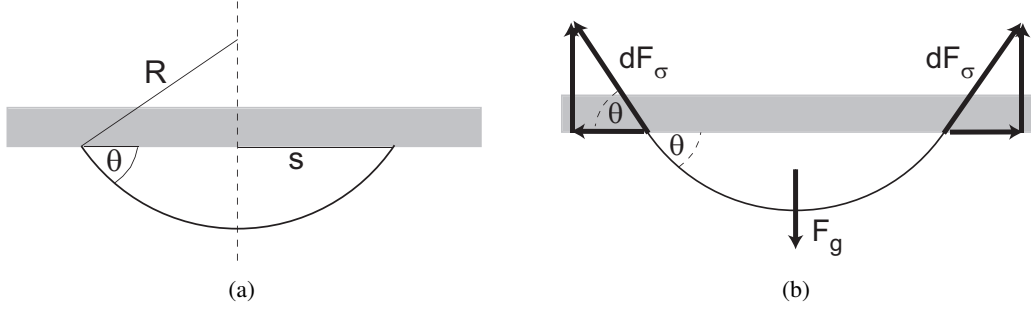


Figure 1: (a) Droplet hanging down from a horizontal plane.

(b) Forces acting on the droplet. F_g denotes the force of gravity, F_σ the force due to the surface tension of the water/air-interface at the contact line. Notice that the vectors $d\mathbf{F}_\sigma$ represent infinitesimal forces contributed by two infinitesimal elements of the contact line. Because these are diametrically located, the horizontal component of F_σ vanishes if integrated around the circular contact line. The vertical component of F_σ may surmount F_g , in which case the droplet remains attached to the horizontal plane. For $F_\sigma < F_g$ the droplet falls down.

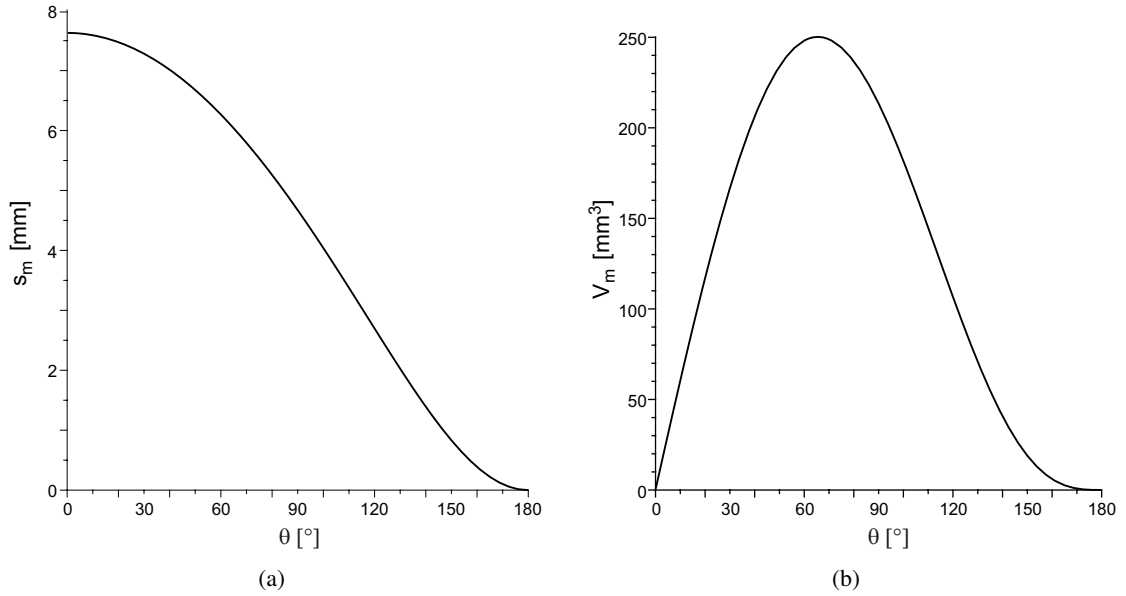


Figure 2: (a) Contact circle radius $s_m(\theta)$ related to the maximum volume of a droplet as a function of contact angle θ . The maximum of $s_m(\theta)$ is located at $\theta_{s_m} = 0^\circ$ (see (10)).

(b) Volume $V_m(\theta)$ related to the maximum volume of a droplet as a function of contact angle θ . The maximum of $V_m(\theta)$ is located at $\theta_{V_m} \approx 65.5^\circ$ (see (12)).

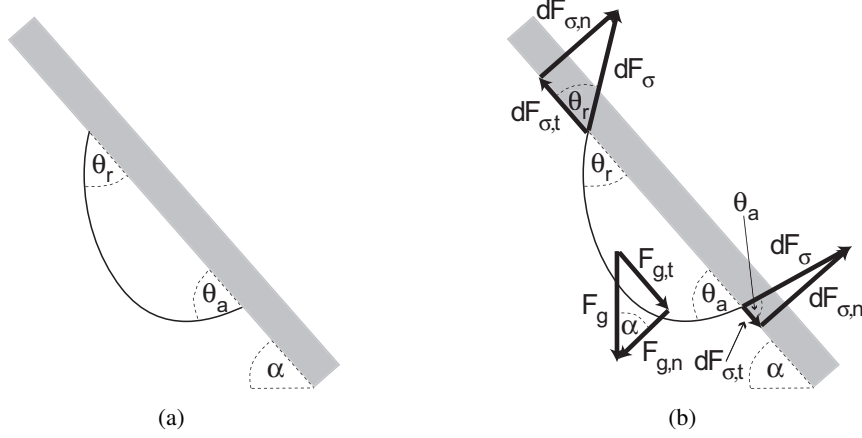


Figure 3: (a) Droplet hanging down from a plane which is inclined against the horizontal by an angle α . θ_r and θ_a denote the receding and advancing contact angle, respectively. (b) Forces acting on a droplet hanging down from a plane which is inclined against the horizontal by an angle α . θ_r and θ_a denote the receding and advancing contact angle, respectively. \mathbf{F}_g denotes the force of gravity, \mathbf{F}_σ the force due to the surface tension of the water/air-interface at the contact line. Subscripts n and t denote normal and tangential components with respect to the plane. Because the infinitesimal force vectors $d\mathbf{F}_\sigma$ are oriented tangentially to the water/air-interface, the inequality $\theta_r \neq \theta_a$ implies that the magnitude of their (infinitesimal) components parallel and normal to the plane vary along the contact line.

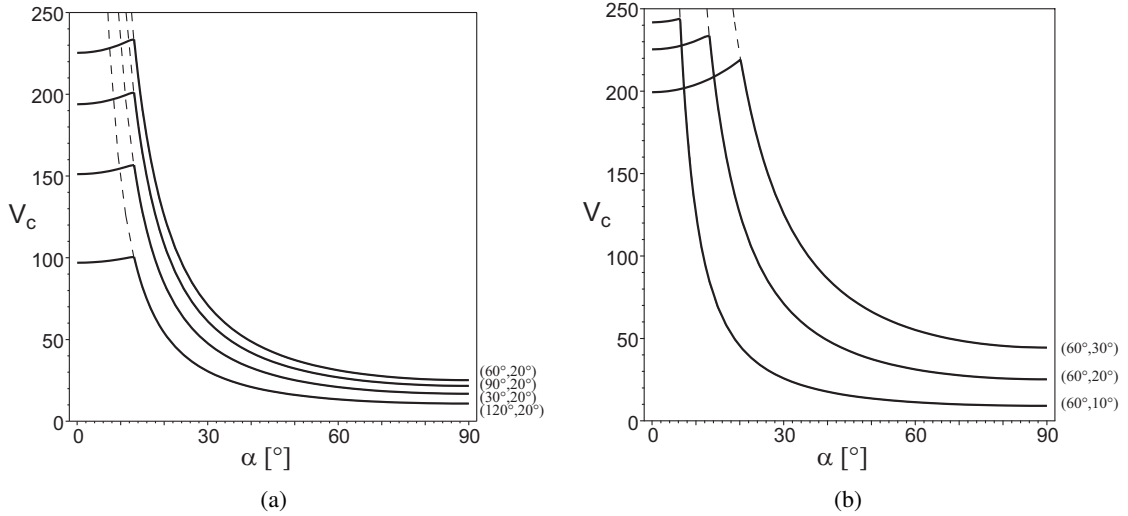


Figure 4: Critical Volume V_c of a hanging droplet (solid lines) and of a sitting droplet (broken lines) as a function of the inclination angle α . Droplets characterised by (V, α) -pairs lying below a curve (V denotes the volume of the droplet) remain immobile, whereas droplets characterised by a (V, α) -pair above this curve either detach from the leaf and fall down (curve segments to the left of the cusps) or slide down while keeping contact with the inclined leaf (curve segments to the right of the cusps). (a) The different curves are generated by insertion of the values $(\theta, \chi) = (60^\circ, 20^\circ)$, $(90^\circ, 20^\circ)$, $(30^\circ, 20^\circ)$ and $(120^\circ, 20^\circ)$ (from top to bottom) into expression (22). (b) The different curves are generated by insertion of the values $(\theta, \chi) = (60^\circ, 30^\circ)$, $(60^\circ, 20^\circ)$ and $(60^\circ, 10^\circ)$ (from top to bottom) into expression (22).

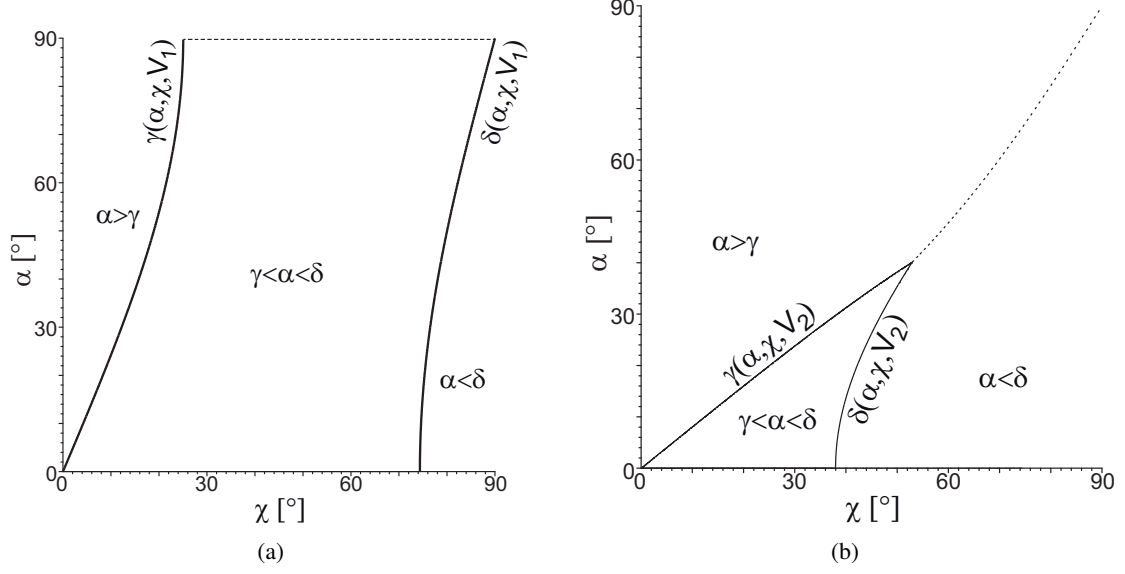


Figure 5: Areas of moving ($\alpha > \gamma$ and $\alpha < \delta$) and immobile ($\gamma < \alpha < \delta$) droplets hanging from a plane which is inclined against the horizontal by an angle α . χ denotes the half-difference of advancing and receding contact angle. $\gamma(\alpha, \chi, V)$ and $\delta(\alpha, \chi, V)$ denote gliding angle and “detachment angle” defined in equations (24) and (25). Immobile droplets are related to (χ, α) -pairs lying within the tetragon. Droplets characterised by (χ, α) -pairs outside the tetragon either slide down (area denoted $\alpha > \gamma$) or detach from the plane and fall down (area denoted $\alpha < \delta$).

(a) For $V_1 = 0.14 V_m < (2/\pi)^{3/2} V_m$ the curves $\gamma(\alpha, \chi, V_1)$ and $\delta(\alpha, \chi, V_1)$ form a “tetragon of immobility” which covers the complete interval $0 < \alpha < \pi/2$. Hence, by adjusting χ appropriately, a droplet of this volume can be made to adhere to an arbitrarily inclined plane.

(b) For $V_2 = 0.7 V_m > (2/\pi)^{3/2} V_m$ the curves $\gamma(\alpha, \chi, V_2)$ and $\delta(\alpha, \chi, V_2)$ intersect and form a “triangle of immobility” which covers only part of the interval $0 < \alpha < \pi/2$. Hence, droplets of this volume cannot be kept immobile for every inclination $0 < \alpha < \pi/2$, even if χ can be arbitrarily chosen. The broken curve indicates whether a droplet slides down ($\alpha > \gamma$) or detaches ($\alpha < \delta$) from the plane.

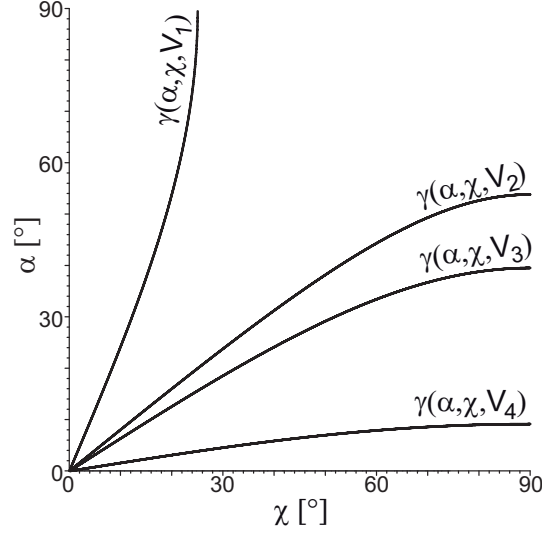


Figure 6: Areas of moving and immobile droplets sitting on a plane which is inclined against the horizontal by an angle α . χ denotes the half-difference of advancing and receding contact angle. The curves $\gamma(\alpha, \chi, V_k)$ ($k = 1 \dots 4$) represent the gliding angle defined in equation (24) for the droplet volume V_k . Immobile droplets are related to (χ, α) -pairs lying above/to the left of a curve related to a given V_k , droplets characterised by (χ, α) -pairs below/to the right of the same curve slide along the plane. For $V_1 = 0.14 V_m < (2/\pi)^{3/2} V_m$ the curve covers the complete interval $0 < \alpha < \pi/2$. Hence, by adjusting χ appropriately, a droplet of this volume can be made to adhere to an arbitrarily inclined plane. The curves $\gamma(\alpha, \chi, V_k)$ related to $V_2 = 0.7 V_m > (2/\pi)^{3/2} V_m$, $V_3 = V_m$ and $V_4 = 8 V_m$, however, cover only part of the interval $0 < \alpha < \pi/2$. Hence, droplets of these volumes cannot be kept immobile for every inclination $0 < \alpha < \pi/2$, even if χ can be arbitrarily chosen.